Egypt. J. Chem. **Vol. 62**, No. 4 pp. 665 - 678 (2019)

Egyptian Journal of Chemistry
http://ejchem.journals.ekb.eg/

Electrocatalytic Activities of Macro- Porous Nickel Electrode for Hydrogen Evolution Reaction in Alkaline Media

Aliaa A. Mohamed[1] *, Randa M. Abdel-Karim [1], Khaled M. Zohdy [2], Saad. M. El-Raghy [1]

[1]*Corrosion and Surface Treatment Lab, Dept. of Metallurgy, Faculty of Engineering, Cairo University. Giza- Egypt.*

[2]*Higher Technological Institute, 10th of Ramadan City, Egypt.*

ALKALINE water electrolysis is one of the easiest methods for hydrogen production, offering the advantages of simplicity, high purity and low cost. Nickel and other transition metal such as (*Ni, Co, Fe and Mo*) 3 D porous foams are an exciting family of catalysts for hydrogen production in alkaline electrolytes because of their special corrosion resistance and highly intrinsic electrocatalytic activity toward *HER*. In this work, macro porous Ni electrodes have been developed by dynamic hydrogen template electrodeposition *(DHTE)* on stainless steel (AISI 304) substrates. Macro porous Ni electrodes with pore size ranging for 1.3-9.41 *μm* were synthesized by galvanostatic deposition at high current densities. Higher current density and longer deposition time lead to coarsening of pore size obtained. On the other hand, increasing the concentration of NH_4Cl additives lead to a remarkable reduction in pore size. The activity for hydrogen evolution reaction *(HER)* on the obtained layers was evaluated by using potentiodynamic polarization curves and electrochemical impedance spectroscopy *(EIS)* in 10 % KOH solution. The electrochemical tests results showed that Ni deposit with fine pore size (1.7 *μm*) manifests the highest intrinsic activity for *HER*.

Keywords: Electroplating, Metal foams, Dynamic hydrogen template (DHBT), Ni coatings, Micro- porous, water splitting, Hydrogen evolution reaction HER.

Introduction

Hydrogen is considered an ideal energy carrier that can be an alternative to fossil fuels due to the fact that hydrogen is a clean and fully recyclable substance [1,2]. Most of the methods used for H_2 production are based on fossil fuels, due to their easy usage in present designed machines and low costs [3,4]. Nevertheless, it is not consistent with the policies on the way to a green energy system. The electrochemical production of hydrogen by alkaline water electrolysis is one of the most promising methods with great potential of using renewable energy sources [5,6]. Although platinum shows the highest activity for the hydrogen evolution reaction (HER), new electrode materials have been investigated, aiming at the reduction of the cost associated with the electrocatalyst development. Among these materials, nickel and its alloys show a high initial electrocatalytic activity toward the HER [7]. The electrode activity can be enlarged by increasing the real surface area and/or the intrinsic activity of the electrode material [8-10]. In this way, Ni is the most important and studied electrode materials, which respond to their high catalytic activity and stability at low cost [1].

Porous structures, with much larger surface area–to–ratio compared to their fully dense counterparts, are very appealing to enhance certain physical-chemical properties. Nanostructured porous materials have received considerable attention in areas like batteries [11], electro-catalysis [12], super-capacitors [13], or magnetic micro/nanoelectromechanical systems.

Structural electrode, which combines 3D porous morphology, ultra-high surface area, specific crystalline structure, has shown

*Corresponding author e-mail: aliaaabdelfatahmohamed@gmail.com
Received 3/9/2018; Accepted 24/10/2018
DOI: 10.21608/EJCHEM.2018.5017.1443

advantages in electro-catalytic issues due to well controlled structure and composition, which are of paramount importance in electrodes for electrochemical applications [14,15]. Furthermore, they combine these properties with useful characteristics of metals, such as good electrical and thermal conductivity and ductility/ malleability [16]. According to recent researches there are several techniques for the synthesizing of metallic porous structures. There are several methods for porous material production such as Dealloying [17] and dynamic hydrogen template (DHBT) [18] anodization process [19], laser etching [20], combustion synthesis [21], sol–gel technique [22], nano-smelting of hybrid polymer–metal oxide aerogels [23], chemical reduction technique [24] and thermal decomposition process [25].

Dynamic hydrogen template method is considered one of the promising ways to form porous structure metals which formed by hydrogen bubbling that often occurs simultaneously with metal deposition. This process becomes a one-step, low-cost method for the fabrication of NMFs [26-30]. Different working parameters have been controlled in order to enlarge the electrode real surface area, being one of them the electrodeposition at large current densities [31,32].

Macro porous Ni deposits have shown better performance in comparison to the other metal catalysts [33-34]. The present research is focused on further investigation of macro porous Ni deposited at high current density. The effect of current density, deposition time as well as NH_4Cl additive on the deposited layers will be studied. The surface morphology will be examined by means of SEM. The activity towards hydrogen evolution reaction (HER) is assessed by potentiodynamic polarization test and electrochemical impedance spectroscopy (EIS) in alkaline media.

Experimental

Electrodeposition process (DHBT):

Macro porous Ni layers (NMFs) were deposited onto AISI 304 stainless steel electrodes (1 cm^2 area and *2 mm* thickness). These substrate materials were subjected to pre-treatment process (by etching in 37% HCl) for 1 min. Macro porous Ni layers were electrodeposited at current densities of 1 and 1.5 A/cm^2 in a bath composed of $NiCl_2.6(H_2O)$ and NH_4Cl. All chemicals were supplied by (ALPHA CHEMIKA). The bath composition and deposition conditions are summarized in Table 1.

Electrodeposition process was accomplished in one-compartment cell with the substrate surface to be coated in vertical "face-up" position, allowing the free departure of the generated gas bubbles. A large-area graphite electrode of high purity was used as an anode. The experiments were accomplished using dc power supply type Chroma 62000P-100-25 with Chroma 62000P software.

Surface characterization

The structures, morphology and compositions of the developed porous (Ni) deposits were examined by means of a Quanta 250 FEG scanning electron microscope with accelerating voltage 30 K.V, coupled with an Energy-Dispersive X-Ray (EDX) analysis, the pore size measurements were conducted by ImageJ software.

TABLE 1. Chemical composition of electrolytic baths as well as operating condition for electrodeposition of macro porous Ni deposits.

Parameters	Value
Electrolytic bath	
Chemical composition	**Concentration (M)**
$NiCl_2.6(H_2O)$	0.371
NH_4Cl	1, 2, 3
Operating conditions	
Temperature	25° C
pH	3
Current density A/cm^2	1, 1.5
Time, sec	30, 60
Stirring speed, rpm	300

Electrochemical Measurements:

The electrochemical performance of porous Ni deposits was assessed by potentiodynamic polarization test and electrochemical impedance spectroscopy (EIS) using a 3-electrode cell configuration connected to a Gamry instruments potentiostat/galvanostat. The counter-electrode was a platinum electrode, and the reference electrode was calomel electrode. All measurements were carried out in 10% KOH electrolyte at room temperature. For potentiodynamic polarization test, scan rate was 2mV/s and scan range from -0.5 V to 0.5 V with respect to open circuit potential. For the impedance test, the frequency range was: 0.01 Hz- 100 kHz peak-to-peak and amplitude of 10 mV was applied on the open circuit potential. The complex nonlinear least square (CNLS) fitting of the impedance data was carried out with the Gamry Echem software package.

Results and Discussion

Surface characterization

Figures 1, 2 represent SEM macrographs of as-deposited 3D porous Ni film with the addition of 1M of NH_4Cl at different deposition times. The deposited layer presents a foam-like morphology with circular pores, whose sizes range from 1.3 µm to 9.41 µm. Pores with circular shape are seen all over the surface. At current density 1 A/cm^2, increasing deposition time from 30 sec to 60 sec lead to formation of large pore size with lower

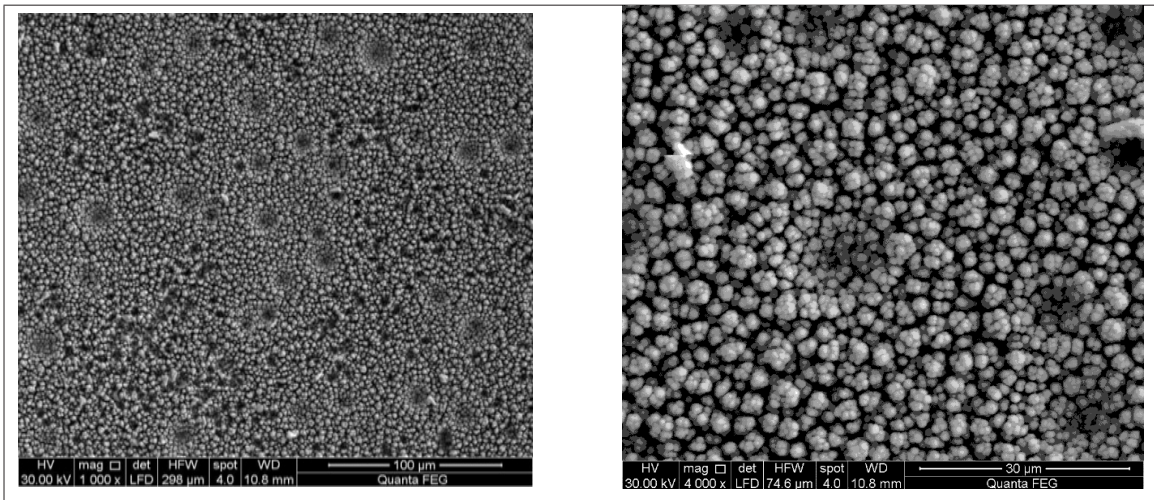

(Low mag.) (High mag.)

- **30 sec**

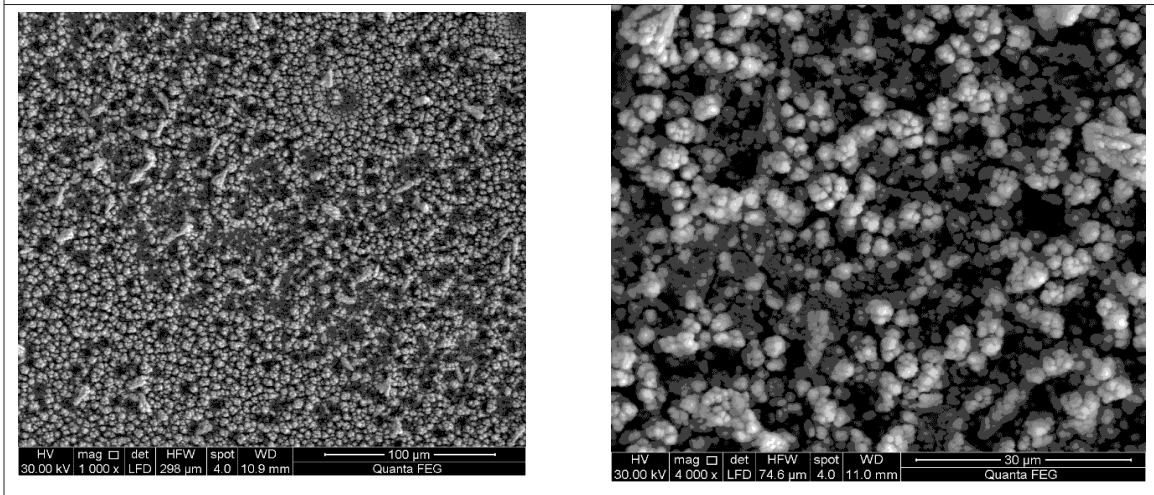

(Low mag.) (High mag.)

- **60 sec**

Fig. 1. SEM micrographs of the macro porous Ni deposits electrodeposited at current density 1A/cm^2, using at 1M NH_4Cl.

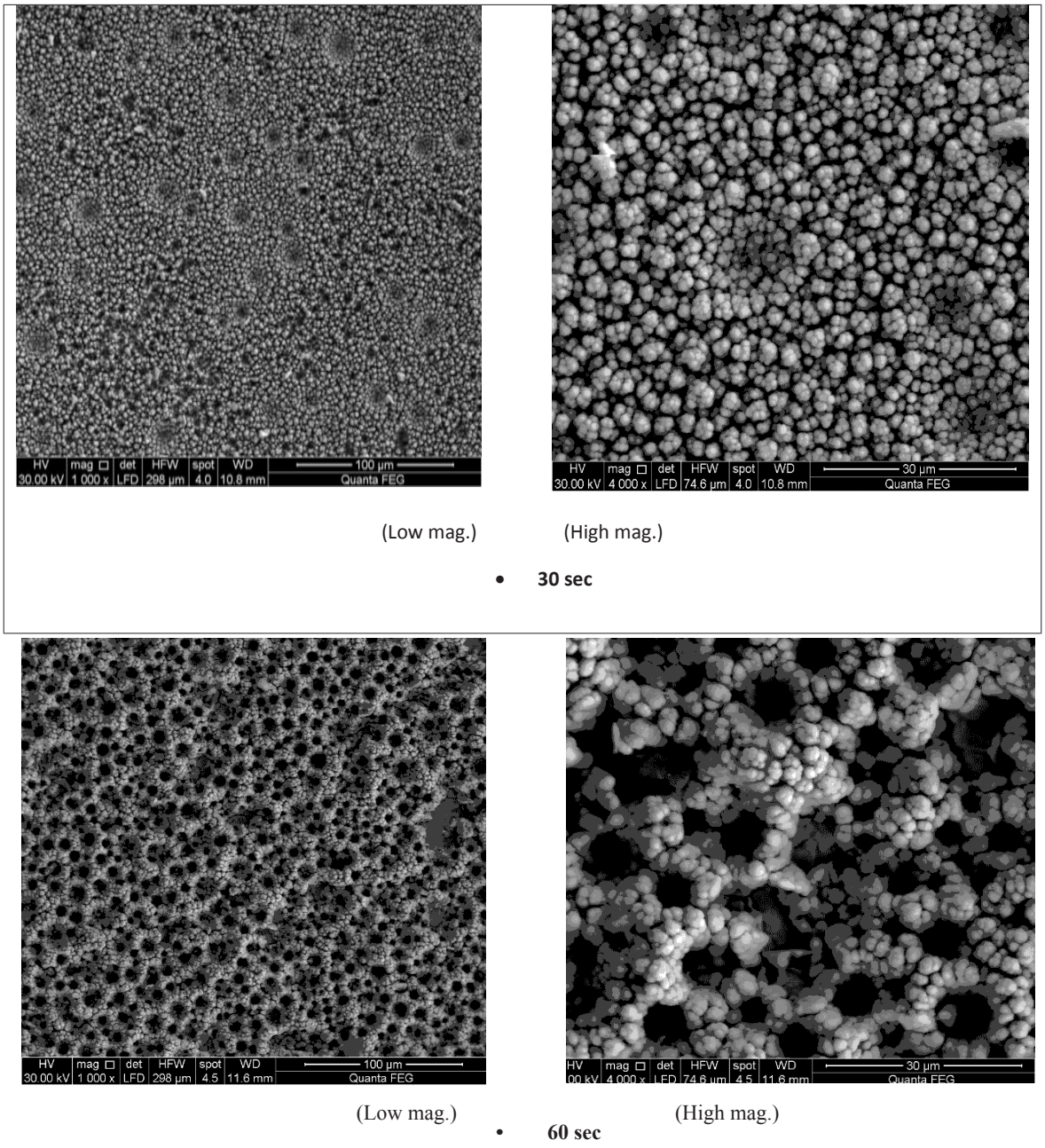

Fig. 2. SEM micrographs of the macro porous Ni deposits electrodeposited at current density 1.5 A/cm², using 1M NH_4Cl.

interspacing between pores. Same trend was observed by increasing the current density from 1A/cm² to 1.5 A/cm².

The effect of increasing NH_4Cl concentration on the morphology of the obtained layers is illustrated in Figure 3. For example, at current density 1.5 A/cm² and deposition time 60 sec, fine pore size with lower interspacing were obtained by increasing NH_4Cl concentration up to 3 M.

The effect of electrodeposition parameters on pore size of macro porous Ni layers is summarized in Table 2. High overpotentials will lead to super-saturation of the solution near the electrode with H_2, resulting in heterogeneous nucleation. The bubble will grow while still in contact with the electrode during its residence time on the surface, with a decreasing contact angle during growth until detachment. Small bubbles in the electrolyte are attracted to the larger bubble and can coalesce [35]. Generally, higher current density and longer deposition time lead to coarsening of pore

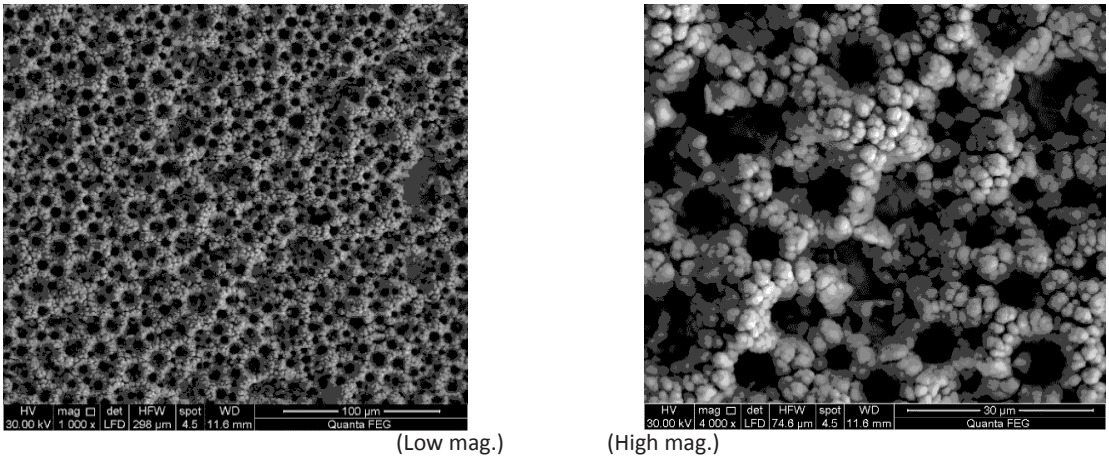

(Low mag.) (High mag.)

- 1 M NH_4Cl

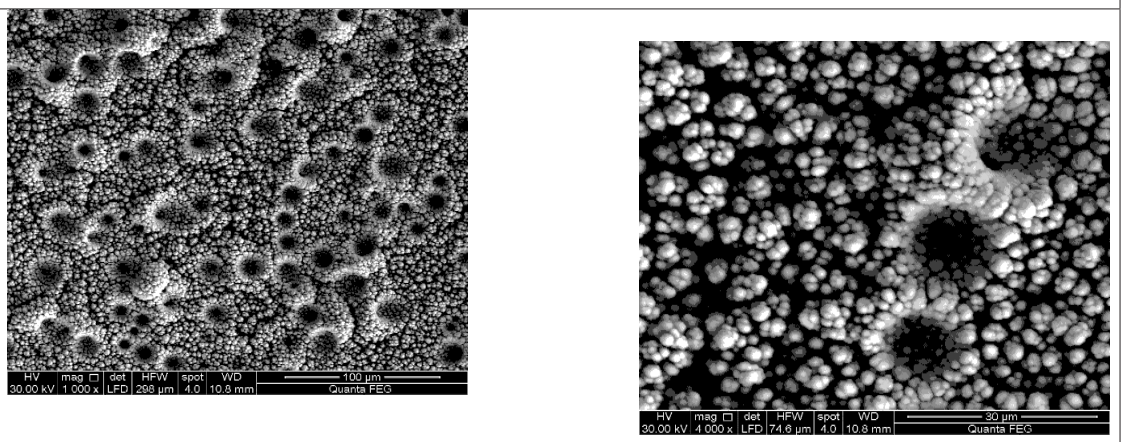

(Low mag.) (High mag.)

- 2 M NH_4Cl

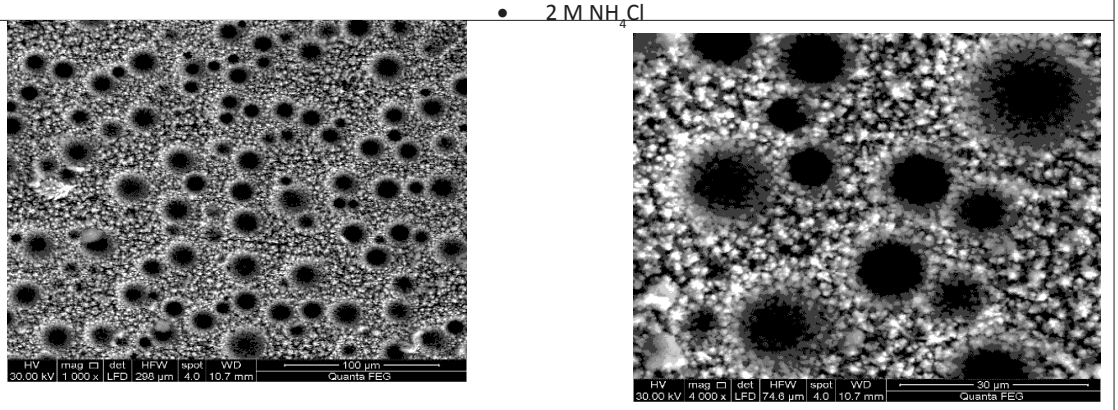

(Low mag.) (High mag.)

- 3 M NH_4Cl

Fig. 3. SEM micrographs of the macro porous Ni deposits electrodeposited at current density 1.5 A/cm^2 and time 60 sec, using different concentration of NH_4Cl

TABLE 2. Pore size of macro porous Ni deposits as a function of electrodeposition parameters.

Working Conditions			Characterization of Deposited Layer
NH_4Cl, M	Current Density, A/cm²	Time, sec	Pore Size (µm)
1	1	30	2.597
		60	4.49
	1.5	30	3.99
		60	7.17
2	1	30	1.3
		60	3.59
	1.5	30	1.7
		60	9.41
3	1	30	3.9
		60	4.5
	1.5	30	3.11
		60	7.28

size obtained. On the other hand, increasing the concentration of NH_4Cl addition lead to a remarkable reduction in pore size.

According to Tsai and co-workers, additives will critically affect bubble behavior, with surfactants residing at the bubble-liquid interface impeding coalescence due to reduced surface tension. Even small surfactant concentrations will have an effect, with large surfactant concentrations preventing coalescence almost completely [36].

Metal electrodeposition can occur around the bubble. The diffusion layer width will decrease due to the hydrodynamic effect of the evolving H_2 [37]. In fact, H_2 evolution has a similar effect on mass transfer as intensive mechanical stirring. The pores in the electrodeposited film will be approximately the same size as the release diameter of the bubbles, with the pore density of the film predominately determined by bubble behavior. Foams with ordered pores were only obtained at ammonium chloride concentrations of 0.5 M and higher. The formation of porous films by dynamic hydrogen electrodeposition also starts at this concentration. Also, the tendency of the pore size decrease with increasing NH^{4+} concentration, as was observed by Serhiy and Chan-Hwa [38].

The finest pore size (1.3 µm) was obtained by electrodeposition at 1 A/cm² for 30 sec with addition of 2 M NH_4Cl.

Electrochemical Measurements

Potentiodynamic test:

Figure 4 illustrates the polarization curves for electrodeposited macro porous Ni layers at different deposition time and current density tested in 10% KOH solution. Table 3 summarizes the electrochemical parameters such as anodic and cathodic tafel plots *(βa* and *βc*), corrosion potential *(Ecorr)*, corrosion current density (icorr), as well as corrosion rate (mm/y). The corrosion rate of electrodeposited macro porous Ni deposits was in the range of (0.077- 2.03 mm/y). The highest corrosion rate (2.03 mm/y) was detected for the macro porous Ni electrode with fine pore size (1.3 µm). This corresponds to deposition current density 1 A/cm² and deposition time 30 sec with addition of 2 M NH_4Cl. On the other hand, the lowest corrosion rate (0.077 mm/y) was obtained at current density 1 A/cm² and deposition time 30 sec with addition of 1M NH_4Cl. The electrocatalytic behavior of macro porous Ni electrodeposited has been evaluated by the comparison of the slope of the cathodic region of tafel polarization curves *(βc)* for the different macro porous Ni deposits. From electrochemical data presented in Table 3, electrocatalytic behavior could be enhanced by decreasing pore size. So that,

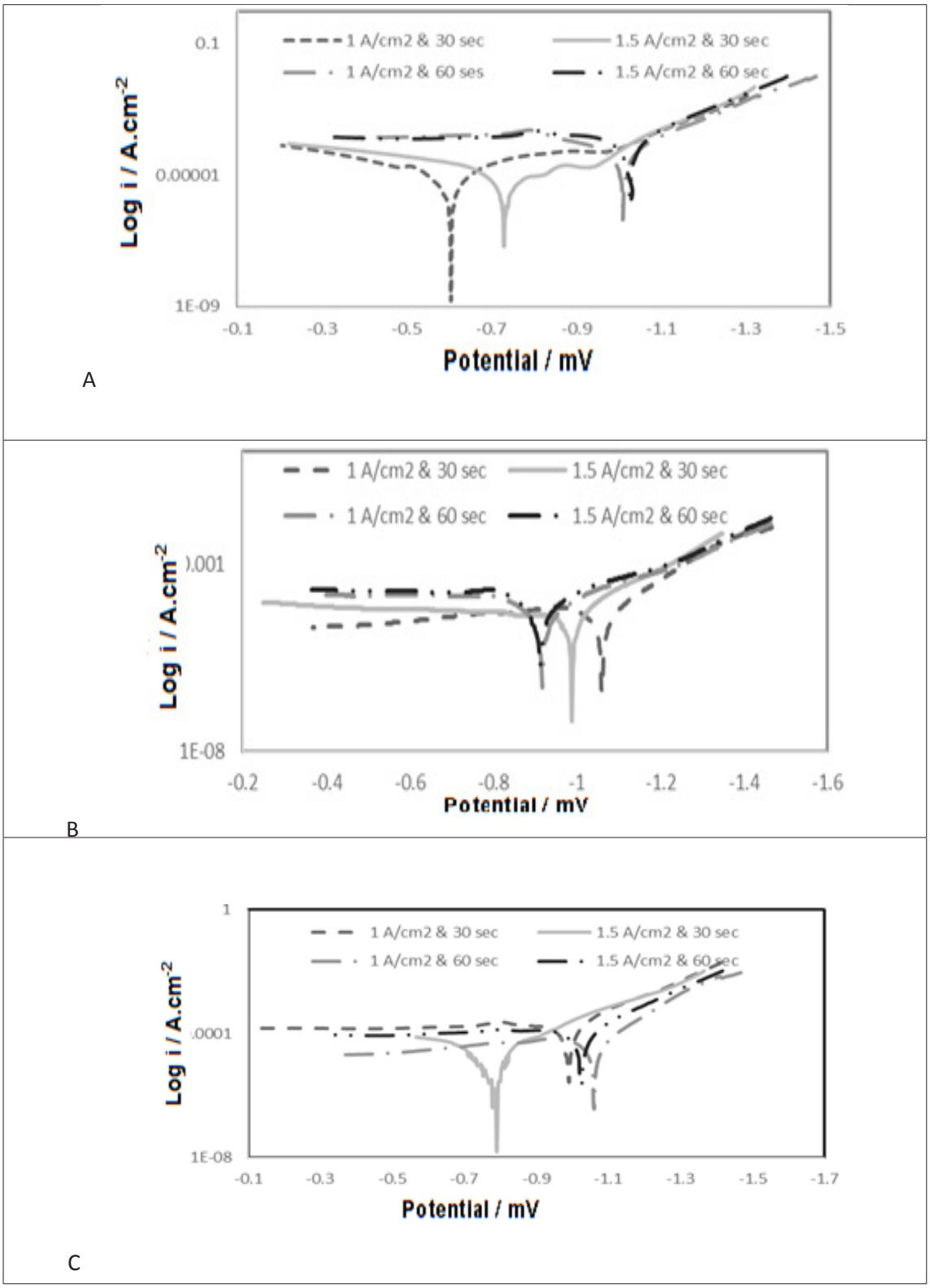

Fig. 4. Potentiodynamic polarization curves obtained in 10% KOH for electrodeposited macro porous Ni deposits in: a) 1 M NH_4Cl, b) 2M NH_4Cl, c) 3M NH_4Cl as a function of electrodeposition parameters.

TABLE 3. Corrosion data obtained from the polarization curves recorded in 10% wt. KOH solutions as function of electrodeposition parameters, for macro porous Ni deposits.

NH_4Cl, M	Current density, A/cm^2	Time, sec	Pore Size (μm)	β_A (mV/decade)	β_C (mV/decade)	I corr (μm)	E corr (mV)	Corrosion rate (mm/y)
1	1	30	2.597	122	93	3.77	-630	0.077
		60	4.49	220	170	70	-1000	1.43
	1.5	30	3.99	95	200	6.1	-729	0.126
		60	7.17	55.4	64.2	15.8	-1030	0.325
2	1	30	1.3	250	225	8.24	-894	2.03
		60	3.59	173	175.8	45.7	-917	0.931
	1.5	30	1.7	200	298	64.1	-947	1.29
		60	9.41	240.9	60	99.2	-911	0.169
1	1	30	3.9	174	170	13.30	-715	0.273
		60	4.5	200	160	33.6	-499	0.689
3	1.5	30	3.11	145.6	110	18.70	-533	0.245
		60	7.28	148	150	4.7	-603	0.097

macro porous Ni electrode with fine pore size (1.3 μm), manifest the highest electrocatalytic activity for hydrogen evolution (βc = 225 mV/decade). According to Abdel-Karim and Halim [10,11], the βc for different nickel-based alloys was in range from 50 to 190. So that micro porous Ni deposits have a high catalytic value as it compares with other works.

Electrochemical impedance spectroscopy measurements (EIS):

Figure 5 shows Nyquist representation data for electrodeposited macro porous Ni layers at different deposition time and current density using 10 wt. % KOH solutions. This figure reveals the presence of two overlapped semicircles. This behavior reported at high frequency indicates the formation of cylindrical pore geometry as it`s observed from *SEM* study [39]. Figures 6 show Bode representation data obtained for electrodeposited macro porous Ni layers in different baths at different deposition time and current density using 10 wt. % KOH solutions. The impedance spectra of the macro porous Ni electrode present two maximum phase angles Bode representation at high frequency. The phase angle of the macro porous Ni electrodes was in the range of 0 to -70 degrees. According to previous work [40-43], this range of phase angle confirms that the Ni deposits have a porous structure. Figure 7 represents the equivalent circuit model of the electrochemical interface used to explain electrocatalytic activity of deposited electrode, where *Ru* is the solution resistance, *Rpo* is the polarization resistance, R_f is the pore Resistance, *Cc* is double layer capacitance, and C_f is the pore capacitance. There is an excellent agreement between the experimental and fitting data.

Table 4 summarizes the data by fitting *EIS* experimental recorded at different deposition parameters, which tested in 10 wt. % KOH solution, of the investigated electrocatalytic coatings.

From this data, it can be observed that the polarization resistance *(Rpo)* increased as the NH_4Cl concentration increased. The macro porous Ni deposit with intermediate pore size (4.49 μm) has the smallest polarization resistance (40 ohm. cm^2).

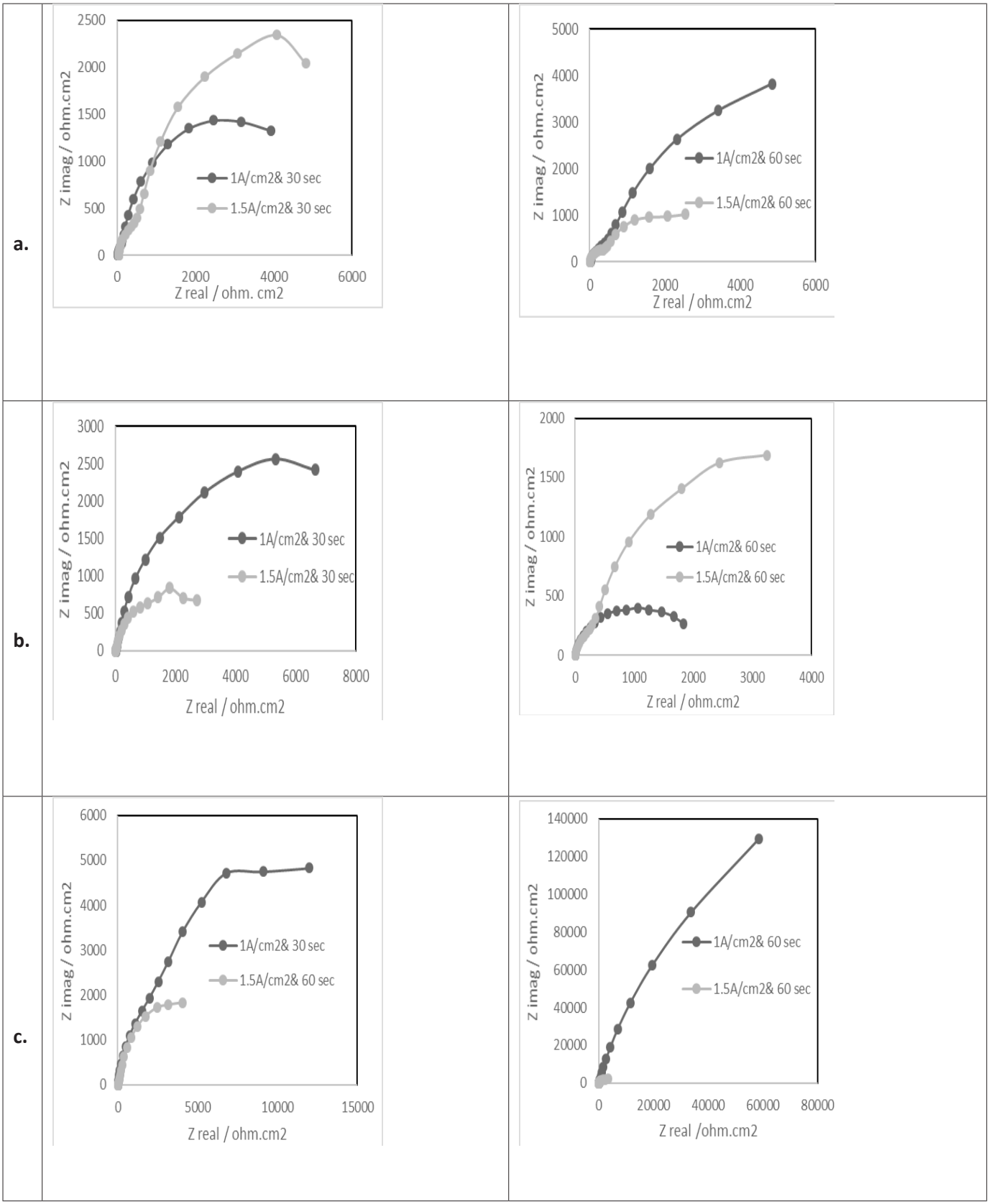

Fig. 5. Nyquist representation data obtained in 10 wt.% KOH solution for electrodeposited macro porous Ni deposits in: a) 1 M NH_4Cl, b) 2M NH_4Cl, c) 3M NH_4Cl as a function of electrodeposition parameters.

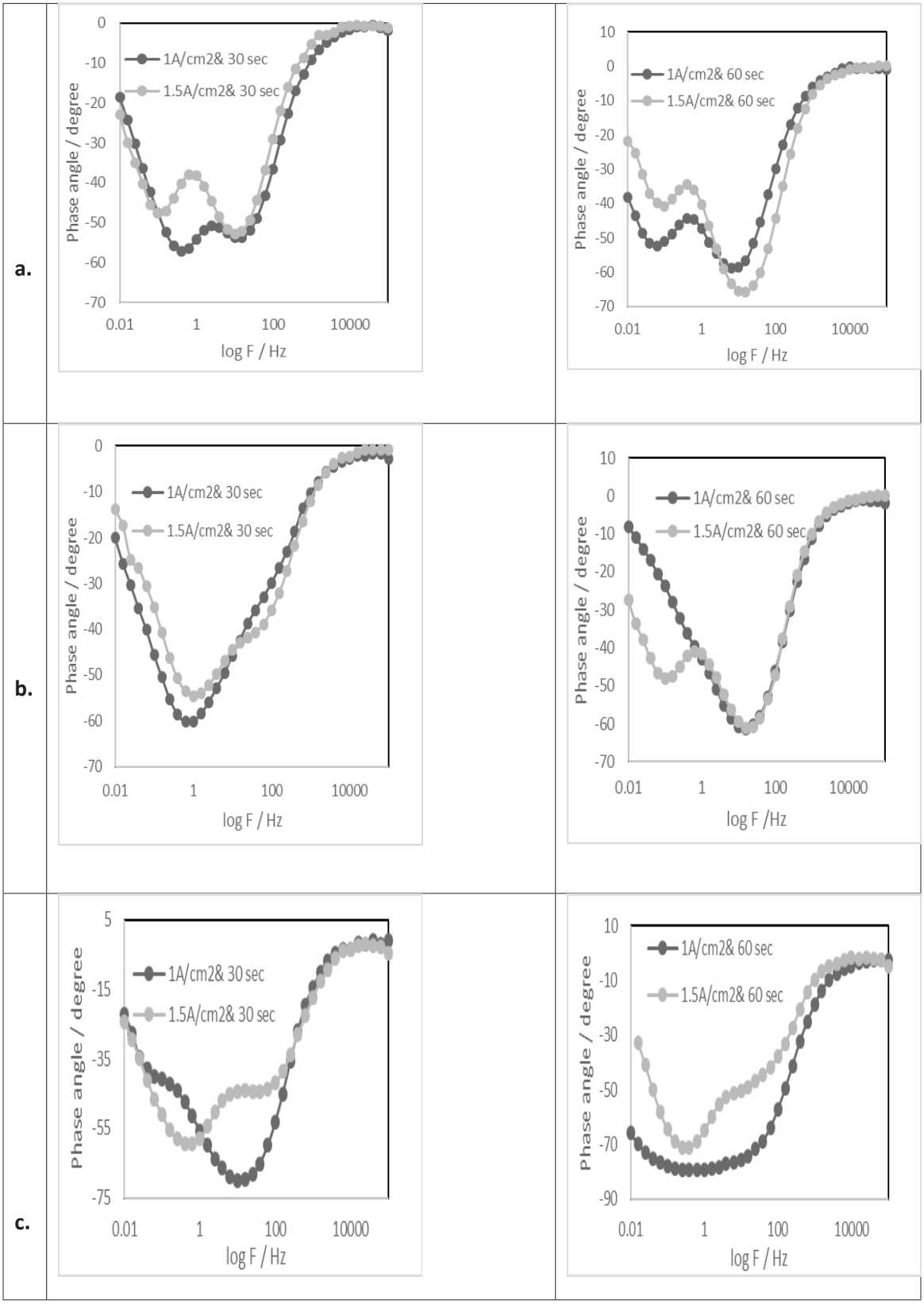

Fig. 6. Bode representation data obtained in 10 wt. % KOH solutions for electrodeposited macro porous Ni deposits in: a) 1 M NH_4Cl, b) 2M NH_4Cl, c) 3M NH_4Cl as a function of electrodeposition parameters.

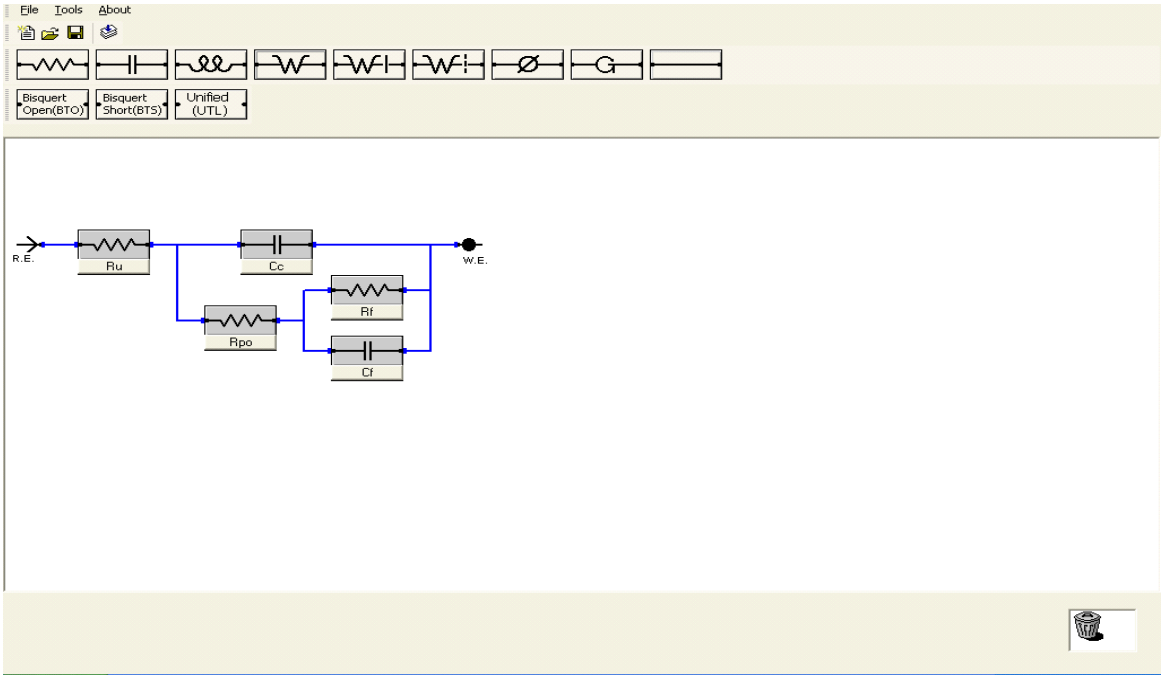

Fig. 7. Equivalent circuit model of the electrochemical interface used to explain the EIS response of the electrocatalytic activity.

TABLE 4. Parameters obtained by fitting EIS experimental spectra recorded in 10% wt. KOH solution as a function of electrodeposition parameters, for macro porous Ni deposits.

NH_4CL, M	Current density, A/cm²	Time, sec	Pore size µm	Rpo kΩ.cm2	Rf KΩ.cm²	Cf µF.cm-2	Ru Ω	Cc µF. cm-2
1	1	30	2.597	0.184	2.863	0.804	11.5	0.171
		60	4.49	0.040	0.7	1.21	12	0.248
	1.5	30	3.99	1	4.5	1.2	15	0.121
		60	7.17	0.577	6	1.306	20	0.170
2	1	30	1.3	0.115	4.33	0.416	20	0.111
		60	3.59	0.310	1.02	0.981	9	0.163
	1.5	30	1.7	0.700	2	2.14	12	0.425
		60	9.41	0.333	3.5	1.719	10	0.158
3	1	30	3.9	3	9.36	0.565	17.05	0.073
		60	4.5	2	6.18	0.644	15	0.101
	1.5	30	3.11	1.2	3.20	1.477	10.32	0.460
		60	7.28	0.8	3.56	0.861	10	0.687

And also observed that, the solution resistance *(Ru)* changed in all the specimens by small degree due to using the same alkaline electrolyte.

The surface area of the fabricated cathodes can also be estimated through the EIS results. The real electrochemically active electrode area, in terms of surface roughness factor *(R_f)* may be determined by means of the quotient between the capacitance of porous and smooth electrodes [42]. In this study, we used a method of evaluating the roughness factor based on the measurement of the double layer capacitance of the macro porous Ni in 10% wt. KOH solution.

From Table 4, it's observed that R_f values decrease with increasing pore size of porous deposits, indicating that H_2 gas bubbles block a fraction of the electrode active surface area, avoiding the electrolyte access. According to Rausch and Pierozynski [43, 44], increasing H_2 gas evolution due to increasing current density will lead to blocking the part of active surface area. So that R_f values decrease with increasing current density and also with increasing pore size.

Macro porous Ni deposits present the highest R_f values in range (from 0.7 to 9 K ohm.cm^2), in the same magnitude order than those reported in research for electrodeposited Raney Ni-Zn [40].

The macro porous Ni electrodeposited from the electrolyte in the presence of a high concentration of NH_4CL have a higher surface area than the ones obtained at a low concentration of ammonia chloride, as shown in Table 4.

It can be concluded that macro porous Ni electrode, with an intermediate R_f (2 k ohm. cm^2) value, manifests the highest apparent and intrinsic catalytic activities (βc = 298 mV/ decade). This corresponds to the following electrodeposition conditions: 1.5 A/cm^2 current density, 30 sec deposition time, and 2M NH_4Cl addition.

Conclusions

Macro porous Ni electrodes with pore size ranging from (1.3) to (9.41) µm were synthesized by galvanostatic deposition (*DHBT*) at high current densities. Higher current density and longer deposition time lead to coarsening of pore size obtained. On the other hand, increasing the concentration of NH_4Cl additives lead to a remarkable reduction in pore size. Despite the high corrosion rate, macro porous Ni electrodes with fine pore size (1.7 µm), with highest βc (298 mV/decade) as well as intermediate surface roughness factor R_f (2 K ohm.cm^2), manifests the highest electrocatalytic activity for HER.

Acknowledgment

This paper is extracted from a Ph. D. thesis submitted to the faculty of Engineering-Cairo University as partial fulfillment of the Ph.D. degree.

References

1. Lu J., Xiong T., Zhou W., Yang L., Tang Z. and Chen S., Metal Nickel Foam as an Efficient and Stable Electrode for Hydrogen Evolution Reaction in Acidic Electrolyte under Reasonable Overpotentials, *ACS Appl Mater, A-E* (2016).
2. Sohair A. S., Reham M.M., Ghada M. M. and M.M. Selim, Production of Hydrogen from Industrial Metal Waste, *Egypt. J. Chem.,* **58,** 5, 555 -561 (2015).
3. Hosseini S. and Wahid M., Hydrogen production from renewable and sustainable ene0rgy resources: promising green energy carrier for clean development, *Renew Sust Energ Rev,* **57,** 850-866 (2016).
4. Li Y., Yang S., Li H., Li G., Li M., Shen L., Yang Z. and Zhou A., Electrodeposited ternary iron-cobalt-nickel catalyst on nickel foam for efficient water electrolysis at high current density, *Colloids and Surfaces A: Physicochem Eng. Asp,* **506,** 694–702 (2016).
5. Gonza´lez-Buch C., Herraiz-Cardona I., Ortega E., Garcı´a-Anto´n J. and Pe´rez-Herranz V., Synthesis and characterization of macro porous Ni, Co and Ni electrocatalytic deposits for hydrogen evolution reaction in alkaline media, *Int J Hydrogen Energy,* **38,** 10157-10169 (2013).
6. Herraiz-Cardona I., González-Buch C., Ortega E., García-Antón J. and Pérez-Herranz. V, Energy Efficiency Improvement of Alkaline Water Electrolysis by using 3D Ni Cathodes Fabricated via a Double-Template Electrochemical Process, *Chem Eng Trans*, **32,** 451-456 (2013).
7. Herraiz-Cardona I., Ortega E., Vázquez-Gómez L. and Pérez-Herranz V., Double template fabrication of three-dimensional macro porous Nickel electrodes for hydrogen evolution reaction, *Int J Hydrogen Energy,* **37,** 2147-2156 (2012).

8. Lai J., Nsabimana A., Luque R. and Xu G., 3D porous carbonaceous Electrodes for electrocatalytic applications, *Joule,* **2,** 1-18 (2012).

9. Abdel-Karim R., Halim J., El-Raghy S., Nabil M. and Waheed A., Surface morphology and electrochemical characterization of electrodeposited Ni–Mo nanocomposites as cathodes for hydrogen evolution, *J Alloy Compd,* **530,** 85-90 (2012).

10. Halim J., Abdel-Karim R., El-Raghy S., Nabil M. and Waheed A., Electrodeposition and characterization of nanocrystalline Ni-Mo catalysts for hydrogen production, *J Nanomater,* 1-9 (2012).

11. Zhang J., Coll M., Puig T., Pellicer E. and Sort J., Conformal oxide nano-coatings on electrodeposited 3D porous Ni films by atomic layer deposition, *J Mater Chem* C, 4, 8655-8662 (2016).

12. Yang F., Cheng K., Xue X., Yin J., Wang G. and Cao D., Nanostructured materials for low temperature fuel cells, *Electrochim Acta,* **107,** 194-199 (2013).

13. Wang G., Liu H., Horvat J., Wang B., Qiao S., Park J. and Ahn H., Highly Ordered Mesoporous Cobalt Oxide Nanostructures: Synthesis, Characterization, Magnetic Properties, and Applications for Electrochemical Energy Devices, *Chem Eur J,* **16,** 11020-11027 (2010).

14. El-Raghy S., Abdel-Karim R., Abdel-Fatah A. and Ahmed H., Study on Nano-deposited Ni-based Electrodes for Hydrogen Evolution from Sea Water Electrolysis, *IJRET,* **2,** 1-15 (2016).

15. Wang G., Zhang L. and Zhang J., A review of electrode materials for electrochemical super-capacitors, *Chem Soc Rev,* **41,** 797–828 (2012).

16. Tappan B.C., Steiner S.A. and Luther E.P., Porous metal foams, *Angew. Chem. Int. Ed,* **49,** 4544–4565 (2010).

17. Fátima Montemor M., Eugénio S., Tuyen N., Silva R. P., Silva T. M. and Carmezim M. J., Nanostructured transition metal oxides produced by electrodeposition for application as redox electrodes for super capacitors, *Nanochem,* 1-27 (2015).

18. Li Y., Fu Z. Y. and Su B. L., Hierarchically structured porous materials for energy conversion and storage, *Adv Fun Mater,* **22**(22), 4634-4667 (2012).

19. Euge´nio S., Silva T., Carmezim M., Duarte R. and Montemor M., Electrodeposition and characterization of nickel–copper metallic foams for application as electrodes for super-capacitors, *J Appl Electrochem,* **44,** 455–465 (2014).

20. Erlebacher J., Aziz M., Karma A., Dimitrov N. and Sieradzki K., Evolution of nano porosity in dealloying, *Nature,* **410,** 450–453 (2001).

21. Abdel-Karim R. and El-Raghy S., Electrochemical deposition of porous metallic foams for energy applications, *Adv Mater Appl: Micro to Nano Scale,* One Central Press, Chapter 4, 69-91 (2017).

22. Mott D., Luo J., Njoki P., Lin Y., Wang L. and Zhong C., Synergistic activity of gold-platinum alloy nanoparticle catalysts, *Catal. Today,* **122,** 379- 385 (2007).

23. Vega A. and Newman R., Porous metals fabricated through electrochemical dealloying of Ag-Au-Pt with systematic variation of Au to Pt ratio, *J Electrochem. Soc.,* **161,** C1- C10 (2014).

24. Kumar A., Yadav N., Bhatt M., Mishra N., Chaudhary P. and Singh R., Sol-Gel Derived Nanomaterials and It's Applications: A Review, *Res J Chem Sci,* **12,** 98-105 (2015).

25. Leventis N., Chandrasekaran N., Sadekar G., Sotiriou-Leventis C. and Lu H., One-photosynthesis of interpenetrating inorganic/organic networks of CuO/resorcinol-formaldehyde aerogels: nanostructured energetic materials, *J Am Chem Soc,* **131,** 4576–4577 (2009).

26. Avisar-Levy M., Levy O., Ascarelli O., Popov I. and Bino A., Fractal structures of highly-porous metals and alloys at the nanoscale, *J Alloy Compd,* **635,** 48–54 (2015).

27. Zhang X., Guan P., Malic L., Trudeau M., Rosei F. and Veres T., Porous twinned Pt-Pd with highly catalytic activity and stability, *J Mater Chem* A., **3,** 2050–2056 (2015).

28. Silva R., Eugénio S., Silva T., Carmezim M. and Montemor M., Fabrication of three-dimensional dendritic Ni–Co films by electrodeposition on stainless steel substrates, *J Phys Chem C,* **116,** 22425–2243 (2012).

29. Nikolic´ N., Popovb K., Pavlovića L. and Pavlović M., Morphologies of copper deposits obtained by *the electrodeposition at high overpotentials, Surf Coat Tech,* **201,** 560–566 (2006).

30. 30. Shin H.C. and Liu M., Copper foam structures

with highly porous nanostructured walls, *Chem Mater,* **16,** 5460–5464 (2004).

31. Shin H.C., Dong J. and Liu M., Porous structures prepared by an electrochemical deposition process, *Adv Mater,* **15,** 1610–1614 (2003).

32. Nikolic` N., Fundamental aspects of copper electrodeposition in the hydrogen co-deposition range, *Zastita Materijala,* **51,** 197–203 (2010).

33. Herraiz-Cardona I., Ortega E., Garcı´a-Anto´n J. and Pe´rez- Herranz V., Assessment of the roughness factor effect and the intrinsic catalytic activity for hydrogen evolution reaction on Ni-based electrodeposits, *Int J Hydrogen Energy,* 36, 9428- 9440 (2011).

34. Hiraiwa C., Okuno K., Tawarayama H., Majima M., Nishimura J. and Tsuchida H., Application of Ni Porous Metal to Solid Oxide Fuel Cells, *IJEE,* **83**, 59-65 (2016).

35. Matsushima H., Kiuchi D., Fukunaka Y. and Kuribayashi K., Single bubble growth during water electrolysis under microgravity, *Electrochem Commun,* **11,** 1721–1723 (2009).

36. Tsai W. L., Hsu P. C., Hwu Y., Chen C. H., Chang L. W., Je J. H., Lin H. M., Groso A. and Margaritondo G., Electrochemistry: building on bubbles in metal electrodeposition, *Nature,* **9,** 417, 139 (2002).

37. Janssen L. J. and Hoogland J., The electrolysis of an acidic NaCl solution with a graphite anode III. Mechanism of chlorine evolution, *Electrochim. Acta,* **15**, 941-951 (1970).

38. Cherevko S. and Chung C. H., Impact of key deposition parameters on the morphology of silver foams prepared by dynamic hydrogen template deposition, *Electrochem Acta,* **55,** 6383–6390 (2010).

39. Levie R., Electrochemical responses of porous and rough electrodes. In: Delahay P, Tobias CW, editors. *Adv Electrochem Eng*, vol. 6. Interscience; p: 329-97 (1967).

40. Chen L. and Lasia A., Study of the kinetics of hydrogen evolution reaction on nickel-zinc powder electrodes. *J Electrochem Soc,* **139**, 3214-9 (1992).

41. Keyser H., Beccu K. and Gutjahr M., Estimation of the pore structure of porous electrodes by impedance measurements, *Electrochem Acta*, **21,** 539-43 (1981).

42. Rausch S. and Wendt H., Morphology and utilization of smooth hydrogen-evolving Raney nickel cathode coatings and porous sintered-nickel cathodes, *J Electrochem Soc,* **143,** 2852-62 (1996).

43. Pierozynski B. and Smoczynski L., Kinetics of hydrogen evolution reaction at nickel-coated carbon fiber materials in 0.5 M H_2SO_4 and 0.1 M NaOH solutions, *J Electrochem Soc*, **156,** B1045-50 (2009).

44. Yu L., Lei T., Nan B., Jiang Y., He Y. and Liu C., Characteristics of a sintered macro porous Ni-Cu alloy cathode for hydrogen production in a potassium hydroxide solution, *Energ,* **97,** 498-505 (2016).

النشاط الكهربي لقطب النيكل المسامي لانتاج الهيدروجين في الوسط القاعدي

علياء عبد الفتاح محمد[1]، راندا محمد عبد الكريم[1]، خالد محمد زهدي[2]، سعد مجاهد الراجحي[1]

[1]معمل التاكل والسطوح - قسم الفلزات - كلية الهندسة - جامعة القاهرة - الجيزة - مصر.

[2]المعهد العالي للتكنولوجيا - العاشر من رمضان - مصر.

يعد التحليل الكهربائي للمياة القلوية احد اسهل الطرق لانتاج الهيدروجين، مما يوفر مزايا البساطة والنقاء العالي والتكلفة المنخفضة. يعتبر النيكل المسامي والمعادن الانتقالية الاخري احد العوامل الحفازة لانتاج الهيدروجين بسبب مقاومتهم الخاصة للتاكل، ولديها نشاط كيميائي قوي تجاه انتاج الهيدروجين.

في هذا البحث تم انتاج قطب النيكل المسامي عن طريق الطلاء الكهربي علي سطح من الحديد(AISI304) حيث وجد فيها حجم المسام يتراوح مابين 1.3 الي 9.41 ميكرون. ووجد ايضا ان عند زيادة التيار الكهربي وزيادة وقت الترسيب يؤدي الي كبر حجم المسامات الموجودة علي السطح.

ومن ناحية اخري زيادة تركيز كلوريد الامونيوم يؤدي الي انخفاض ملحوظ في حجم المسام.

و بدراسة النشاط الكيمائي للاقطاب وجد ان طبقة النيكل المسامية التي يبلغ حجم المسام فيها الي 1.7 ميكرون هي الطبقة ذات الاعلي نشاط لانتاج الهيدروجين في الوسط القاعدي.